PROCEEDINGS, Thirty-Fourth Workshop on Geothermal Reservoir Engineering
Stanford University, Stanford, California, February 9-11, 2009
SGP-TR-187

ELECTRICAL RESISTIVITY IMAGE OF THE KIZILDERE GEOTHERMAL SYSTEM INFERRED FROM MAGNETOTELLURIC DATA

Murat BAYRAK[1], Umran SERPEN[2], O.Metin ILKIŞIK[3]

[1]Istanbul University, Engineering Faculty, Geophysical Eng. Dept., Avcilar Campus,
34320 Istanbul, Turkey
[2]Istanbul Technical University, Mining Faculty, Petroleum and Natural Gas Eng. Dept. Maslak Campus,
34469, Istanbul, Turkey
[3]Anadolu Yerbilimleri, Perpa-A Blok, Kat: 5, #157, Sisli,
34354 Istanbul, Turkey

e-mail: serpen@itu.edu.tr

ABSTRACT

A MT survey was conducted to identify conductive zones inside metamorphic complex in the easternmost part of B. Menderes Graben. In this study, using this surveying data, creation of some images of the shallow and deeper parts of the area was aimed. Broadband (200-0.002 Hz) magnetotelluric data were acquired along seven profiles crossing the B. Menderes Graben with a total of 22 MT stations. These data were modeled using two-dimensional inverse techniques. The main findings are: (1) presence of wide conductive regions with very low resistivity (<20 ohm m) were imaged at depth of ~2 km, extending to maximum ~5 km depth, and these conductive regions signify potential geothermal resource in the area, (2) presence of deep conductive regions (<75 ohm m) at a depth from ~ 30 km to 40 km, which reflects shallow asthenosphere, were correlated with the presence of high enthalpy geothermal system and its heat source.

INTRODUCTION

The Kizildere geothermal field, which is situated within the MT surveying area, was discovered in 1968, and 17 wells were drilled until mid 1970's assessing the capacity and at the same time developing the field. After a feasibility study, the first geothermal power plant with 17.8 MW_e gross and 15 MW_e rated capacity fed by 6 production wells was installed at the field and power generation started in 1984. Three additional production wells were drilled two years later to supply needed steam to the power plant. A total of 25 wells have been drilled in the field so far. The field has been generating approximately 10 MW_e of energy from year 1984 to 2001. The power plant installed in the field used to generate electricity is a single flash steam with a condensing cycle. A deep well (R-1), was drilled to 2300 m in 1997 for reinjection, but discovered 240^oC temperature. The well R-1 was connected into the production line, and the power production was increased to roughly about 12.5 MW_e. The average geothermal fluid production (nearly at 200^oC) has been 1000 ton/hour. Roughly ¼ of disposal water is currently reinjected into the field through the well R-2 for reservoir pressure maintenance.

GEOLOGICAL SETTING OF SURVEY AREA

Kizildere geothermal field is situated in the northern flank and easternmost part of B. Menderes graben and partly intervened by Çürüksu graben system. It is found in the vicinities of intersection of Gediz graben. In this region a simple stratigraphic section composed of metamorphic basement overlain by Tertiary sediments is found. The stratigraphy is completed by two Quaternary sedimentary formations filling the bottom of the graben. Geothermal area is somehow extended to the south and related strongly to the Tekkehamam geothermal area. There is strong geochemical evidence that these two fields arise from a single geothermal system (Dominco and Samilgil, 1970).

The area between the two grabens is formed by eastern end of Menderes Massif, which is made up by metamorphic rocks of different grade and is partially covered by continental sedimentary formations of Tertiary age. The structural model is completed by a NE-SW regional tectonic feature, characterized by the lowering of its eastern margin that crosses the two grabens and the Massif itself (Enel et al, 1988).

Rising Menderes Massif was first subjected east-west, then north-south extensional regimes and several major grabens (B. Menderes and Gediz) and detachment zones were formed favoring the formation of several geothermal systems in the region. Approximately 50 % higher than the world's average heat flow (Ilkişik, 1995) in the region has also helped the creation of rich geothermal resources.

MAGNETOTELLURIC (MT) METHOD AND DATA ACQUISITION

The MT is the most commonly used method for probing into the deep lithosphere with its low frequency band (10^{-5}-100 Hz). MT is a natural sourced method utilizing the time varying Earth's magnetic field due to electrical storms (for frequencies above 8 Hz) and solar activity (for periods longer than 0.125 s). By Faraday's law of induction, this varying magnetic field induces an electric current and the current generates an electric (telluric) field in the Earth; the strength of the telluric field depends on the conductivity of the medium. In MT method, the time variations of the three components of the magnetic field (H_X, H_Y, H_Z), and the two horizontal components of the Earth's electrical field (E_X, E_Y) are measured on the surface of the Earth (x and y denote northward and eastward directions). The fields are measured in the time domain and are transferred into the frequency domain where cross-spectra are computed, and from these spectra, the MT response function estimates are derived. Horizontal field components are related by the complex MT impedance tensor:

$$\begin{bmatrix} E_X \\ E_Y \end{bmatrix} = \begin{bmatrix} Z_{XX} & Z_{XY} \\ Z_{YX} & Z_{YY} \end{bmatrix} \begin{bmatrix} H_X \\ H_Y \end{bmatrix}$$

In two-dimensional earth case, the on-diagonal impedance elements Z_{XX} and Z_{YY} are zero while principal impedances Z_{XY} and Z_{YX} represent the independent transverse magnetic (TM) and transverse electric (TE) modes of polarizations. The TM mode is defined as having the electric field across strike direction while TE mode has the electric field parallel to strike. The TM mode apparent resistivities (ρ_a) and phases (ϕ) are derived from the non-diagonal elements of the impedance tensor as:

$$\rho_{a,XY}(\omega) = \left(\frac{1}{\omega\mu}\right)\left|Z_{XY}(\omega)\right|^2$$

$$\phi_{XY}(\omega) = \tan^{-1}\left[\frac{\mathrm{Im}\, Z_{XY}(\omega)}{\mathrm{Re}\, Z_{XY}(\omega)}\right]$$

where,

$$Z_{XY}(\omega) = \frac{E_X(\omega)}{H_Y(\omega)}$$

in ohm and $\omega=2\pi f$, μ and f are the magnetic permeability of free space (4π x 10^{-7} H/m) and the frequency in Hz, respectively. Similar expressions apply for TE mode ($\rho_{aYX}(\omega)$ and $\phi_{YX}(\omega)$).

For a uniform earth, the apparent resistivities are true resistivity of the half space, and the phases are 45^o. For a multi-layered earth, apparent resistivity and phase vary with frequency. In MT investigations, short-period MT signals (10^{-4}-10^{-3}) penetrate several hundred meters into the earth whereas long-period signals (10^{3}-10^{4}) penetrate 100 km or more into the upper mantle.

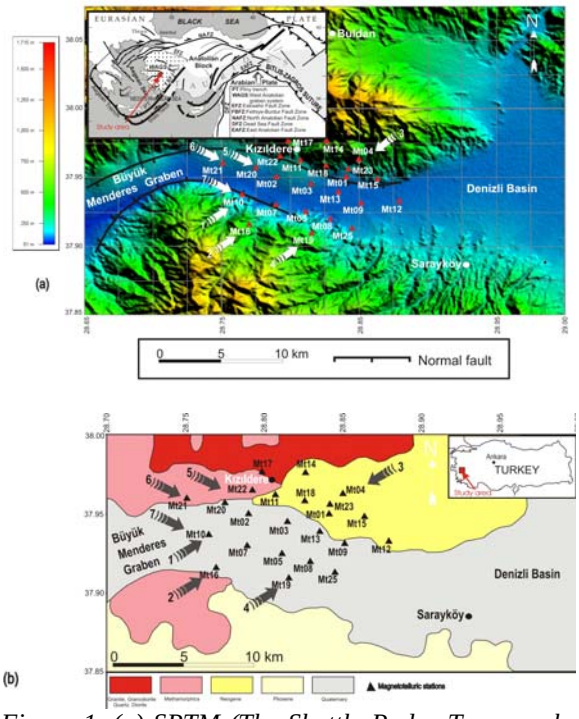

Figure 1. (a) SRTM (The Shuttle Radar Topography Mission) elevation model of study area and main Tectonic elements of Turkey and Mediterranean region. (b) Geology map of the Study area (modified after MTA, 1964) and magnetotelluric site locations (solid three angles) along seven profiles.

The MT measurements discussed here were made at twentytwo locations along a SW-NE direction across western Turkey by Enel et al., (1988), illustrated in Figure 1a and 1b. Only resistivity and phase data were available for this dataset. The MT data were obtained with Cimax Geosystem MT84 MT equipment with frequency range of 0.002-200 Hz. For each station, five components (E_X, E_Y, H_X, H_Y, H_Z) were recorded. The horizontal electric and magnetic field components were measured in the N-S

and E-W directions with a cross-shaped configuration.

Two-dimensional Model

Two-dimensional inversion of the MT dataset was undertaken using the 2-D non-linear conjugate gradient (NLCG) (Mackie et al., 1997; Rodi and Mackie, 2001) inversion method and was performed on twenty-two MT stations. The spread of the "transverse electric" (TE) data for profiles 1, 2, 3, 4, 5, 6 and 7 are about 6.9 km, 9.4 km, 6.2 km, 11.9 km, 6.6 km, 7.6 km and 6.9 km, respectively. Berdicevsky et al. (1998) discussed the relative advantages and disadvantages of the TM and the TE mode data to map geological structures at different depths with different resistivities. They concluded that the TM mode is more sensitive to near surface structures while the TE mode may be more sensitive to deep structures and that the TM mode is more susceptible to static shifts while the TE mode may be almost undistorted. They also showed that the TM mode is more robust to the 3-D effects caused by conductive structures and the TE mode is more robust to the 3-D effects caused by resistive structures. In this study, the data were inverted using TE mode.

The final two-dimensional model was determined by comparing MT parameters calculated from models with estimates provided by the field data. The observed and synthetic resistivity and phase responses from the two-dimensional model on SW-NE are shown in Figure 2, Figure 3, Figure 4 and Figure 5, respectively. Along the profile, the calculated TE values from the model fit well the field data both in terms of apparent resistivity and phase.

Wannamaker et al. (1989) showed that phase data is not affected by local heterogeneities, which causes static shifting. The floor errors of the apparent resistivity and phase data were increased to decrease static-shift effects. The initial model was a 30 ohm m half space. The final resistivity model (Figure 5a, 6a and 7a) has an RMS misfit of 2.06, 1.48, 0.98, 0.99, 1.95, 1.29, and 1.56, respectively.

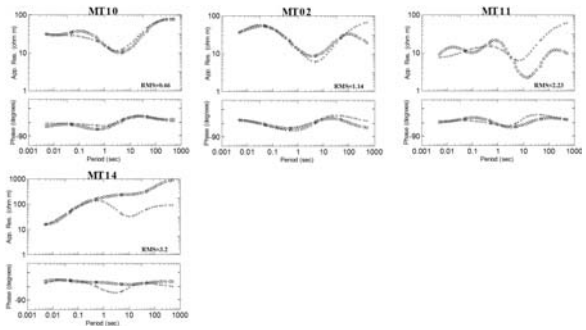

Figure 2. A comparison of the TE response (o) MT data with the model responses from the model given in Figure 6a for profile 1. The RMS misfit for each station for model (Figure 6a) is shown.

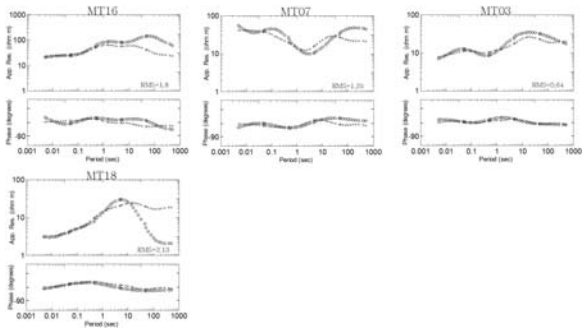

Figure 3. A comparison of the TE response (o) MT data with the model responses from the model given in Figure 7a for profile 2. The RMS misfit for each station for model (Figure 7a) is shown.

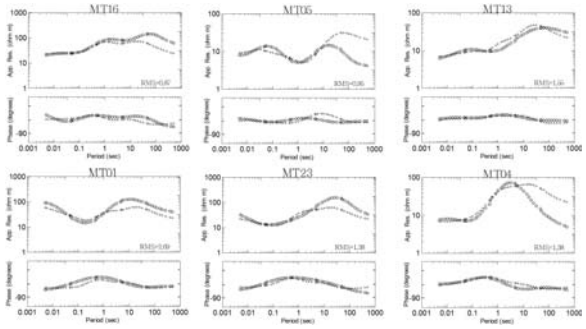

Figure 4. A comparison of the TE response (o) MT data with the model responses (+) from the model given in Figure 8a for profile 3. The RMS misfit for each station for model (Figure 8a) is shown.

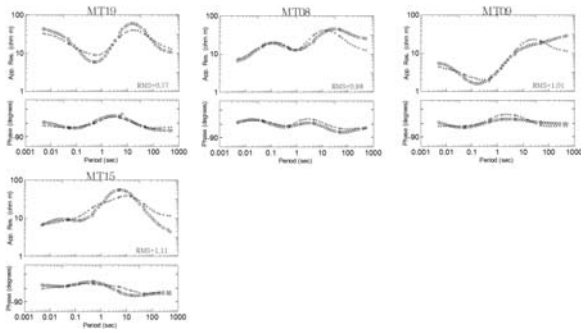

Figure 5. A comparison of the TE response (o) MT data with the model responses from the model given in Figure 9a for profile 4. The RMS misfit for each station for model (Figure 9a) is shown.

If the MT georesistivity models for Profile 1, 2, 3 and 4 given in Figure 6, 7, 8 and 9 are examined following trends are observed:

- Thickness of conductive zones tends to decrease toward northeast. Easternmost well DK-1 well confirms that. In this well relatively moderate temperature was struck (137^{o}C).
- The deepest conductive zones extending to maximum ~5 km depth are found in the midst of the Menderes Graben where thicker upper zones belong to Miocene age sedimentary formations overlain Paleozoic metamorphic series. Very Low resistivity values imply that Miocene sediments are saturated with geothermal fluids in this region.
- Except southwestern MT10 station thicknesses of conductive zones are thinning on graben flanks. That explains successful shallow geothermal wells that are found in the northern flank.
- Unlike other fields that are discovered on the northern flank of B. Menderes Graben, these three profiles indicate both sides of graben flank are active from geothermal point of view. Over twenty wells on northern and one in the southern flank confirm that fact.
- As seen in the first profile, conductive zones in the SW are connected with the other important conductive zone in the midst of B. Menderes graben.
- In the second and the fourth profiles below the north-east region there is a deep conductive zone around 15000 m under northern flank of graben (below MT04). This conductive zone could be the heat source of the geothermal system

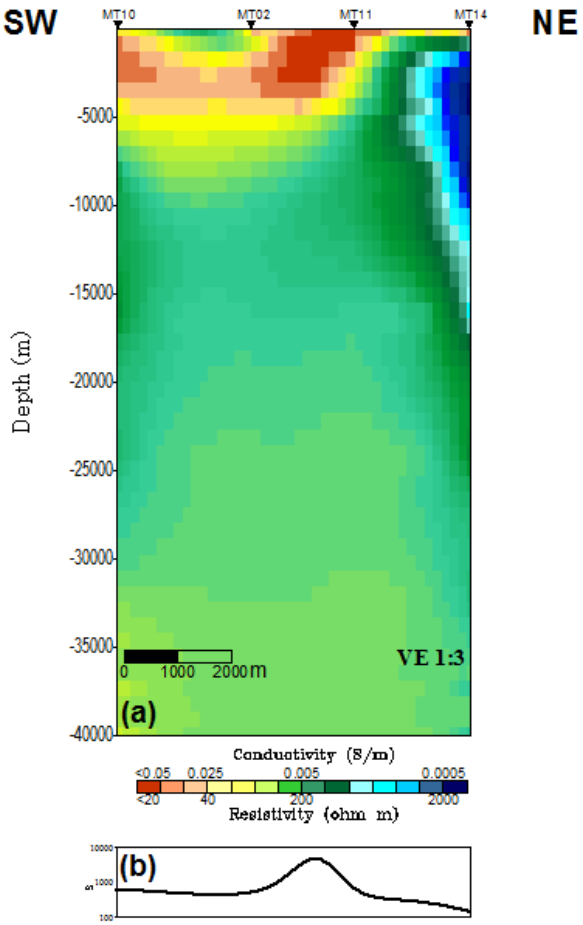

Figure 6. (a) Final MT georesistivity model obtained by 2-D inversion modeling of the MT data along profile 1. The crustal model that is data sensitive to resistivity structures to 40 km is illustrated with 1:3 exaggeration on the figure. (b) The conductance to 40 km.

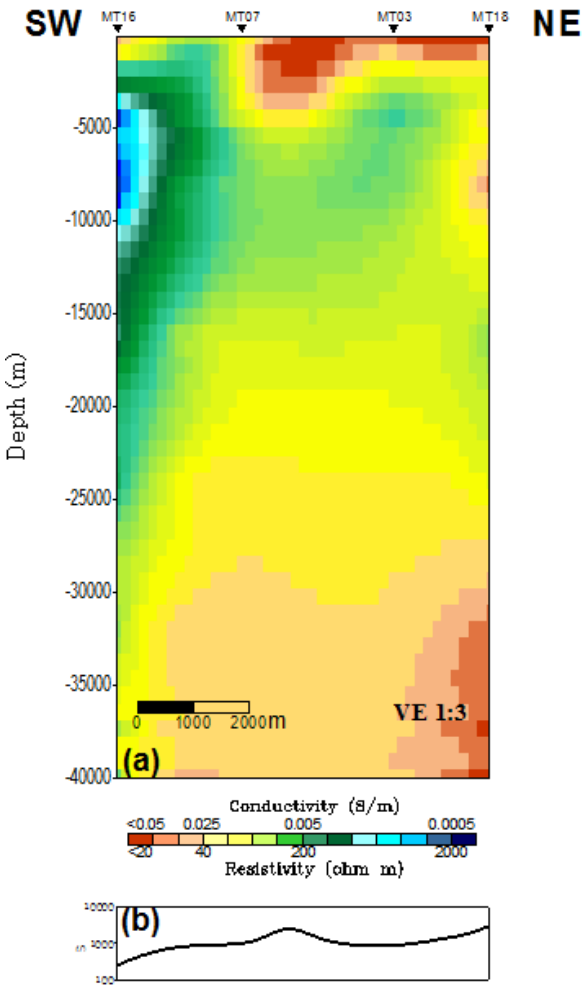

Figure 7. (a) Final MT georesistivity model obtained by 2-D inversion modeling of the MT data along profile 2. The crustal model that is data sensitive to resistivity structures to 40 km is illustrated with 1:3 exaggeration on the figure. (b) The conductance to 40 km.

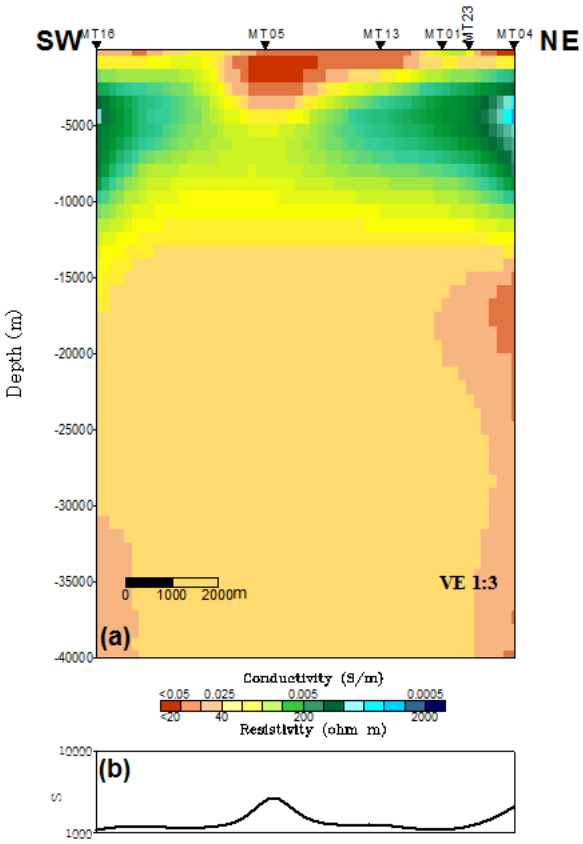

Figure 8. (a) Final MT georesistivity model obtained by 2-D inversion modeling of the MT data along profile 3. The crustal model that is data sensitive to resistivity structures to 40 km is illustrated with 1:3 exaggeration on the figure. (b) The conductance to 40 km.

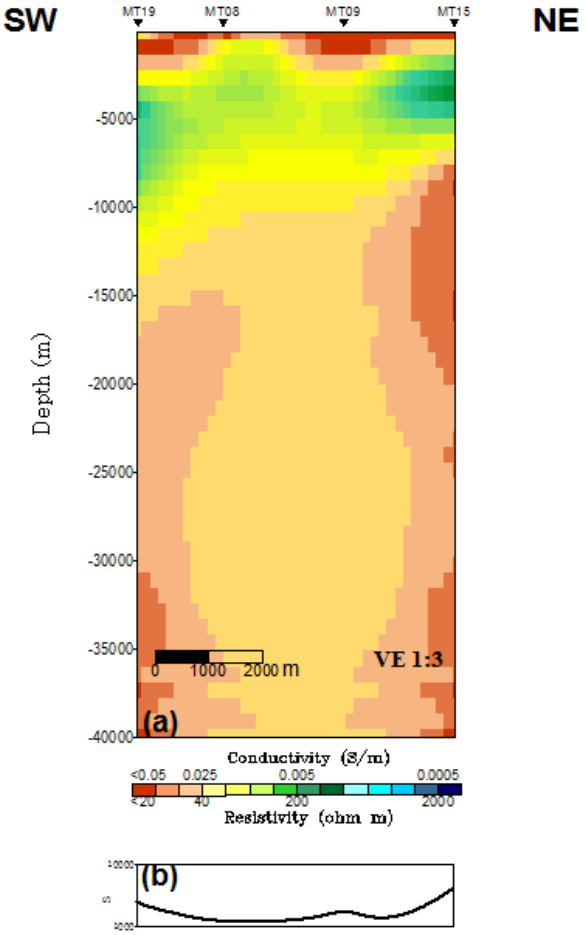

Figure 9. (a) Final MT georesistivity model obtained by 2-D inversion modeling of the MT data along profile 4. The crustal model that is data sensitive to resistivity structures to 40 km is illustrated with 1:3 exaggeration on the figure. (b) The conductance to 40 km.

The observed and synthetic resistivity and phase responses from the two-dimensional model on NW-SE sections are shown in Figure 9, Figure 10 and Figure 11, respectively. Along the profile, the calculated TE values from the model fit well the field data both in terms of apparent resistivity and phase.

After examining MT georesistivity models for the Profiles 5, 6 and 7 given in Figure 13, 14 and 15 following observations are made:

- In all NW-SE profiles conductive zones are thinning toward southeast. DK-1 well confirms that.
- Profile 5 passes over resistive graben structure, but near surface there are conductive zones with thicknesses of 500 m and 1000 m.
- Two intrabasement conductive zones appear at depths approximately 15000 m and 35000 m which also appear in SW-NE profiles 2 and 4. The source of deep conductive zones might be partial melting as a result of shallow asthenospher.
- On profile 6 significant conductive zones with approximately 3000 m thickness are observed in the midst of graben.

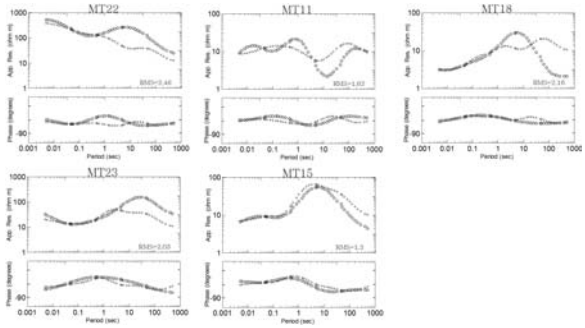

Figure 10. A comparison of the TE response (o) MT data with the model responses (+) from the model given in Figure 13a for profile 5. The RMS misfit for each station for model (Figure 13a) is shown.

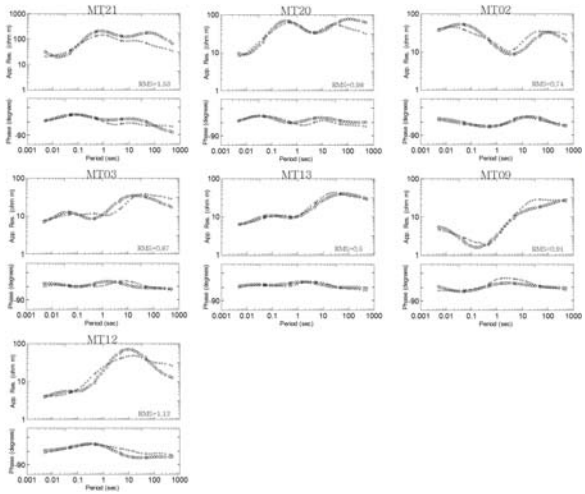

Figure 11. A comparison of the TE response (o) MT data with the model responses from the model given in Figure 14a for profile 6. The RMS misfit for each station for model (Figure 14a) is shown.

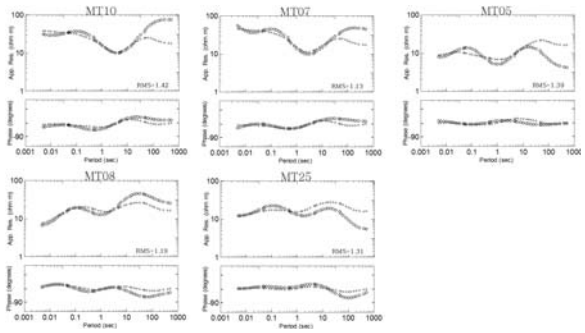

Figure 12. A comparison of the TE response (o) MT data with the model responses from the model given in Figure 15a for profile 7. The RMS misfit for each station for model (Figure 15a) is shown.

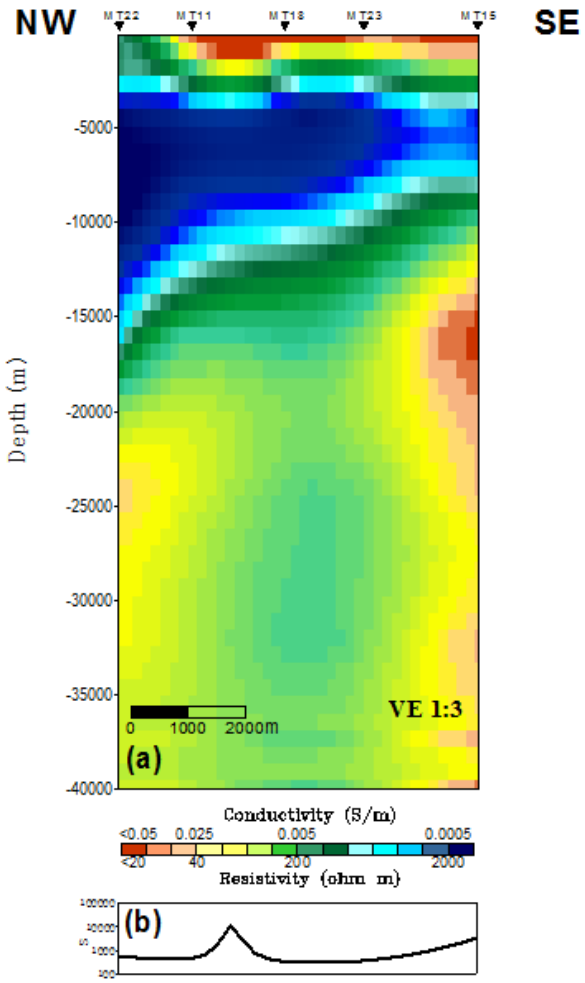

Figure 13. (a) Final MT georesistivity model obtained by 2-D inversion modeling of the MT data along profile 5. The crustal model that is data sensitive to resistivity structures to 40 km is illustrated with 1:3 exaggerations on the figure. (b) The conductance to 40 km.

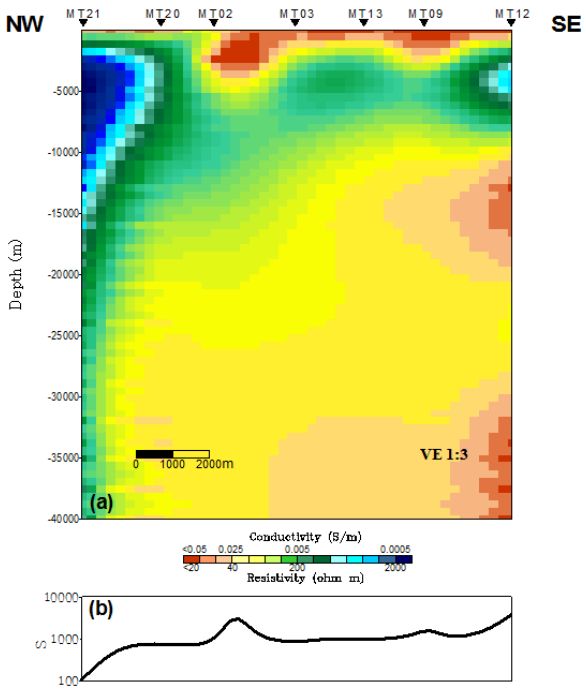

Figure 14. (a) Final MT georesistivity model obtained by 2-D inversion modeling of the MT data along profile 6. The crustal model that is data sensitive to resistivity structures to 40 km is illustrated with 1:3 exaggerations on the figure. (b) The conductance to 40.

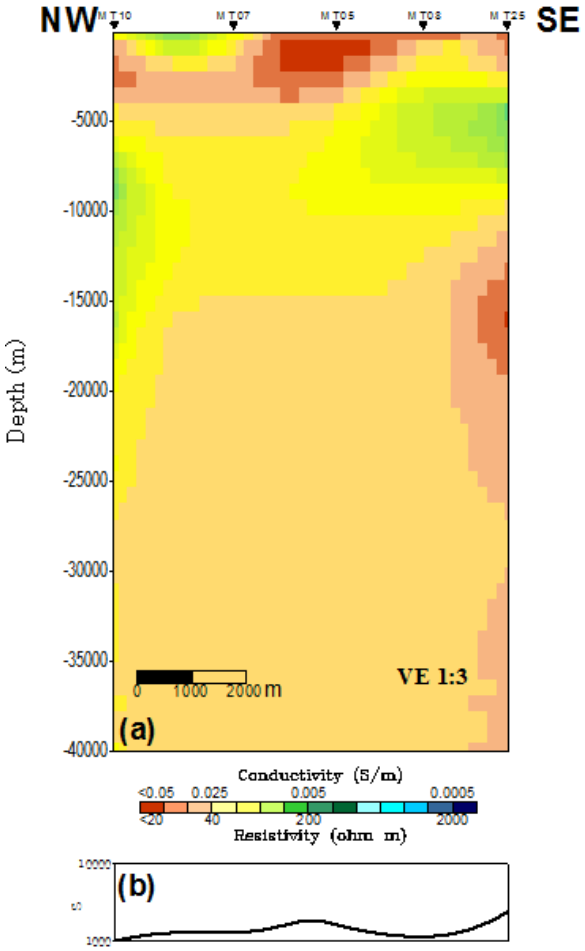

Figure 15. (a) Final MT georesistivity model obtained by 2-D inversion modeling of the MT data along profile 7. The crustal model that is data sensitive to resistivity structures to 40 km is illustrated with 1:3 exaggerations on the figure. (b) The conductance to 40.

CONCLUDING REMARKS

MT transects were built for Kızıldere geothermal field to image geoelectrical resistivity structure of the area.

The 2-D inversion of the TE mode along seven profiles reveal the presence of wide conductive regions with low resistivity (<20 ohm m) at depth of ~2 km, extending to maximum ~5 km depth. This conductive zones looks like low resistive regions studied by Lugão et al. (2002) and Harinarayana et al. (2004) in other geothermal fields.

According to obtained 2-D georesistivity models shallow conductive zones that represent geothermal system extend to both flanks of the B. Menderes Graben, which is unique in the region where several geothermal systems were developed only on the northern flank of the same graben.

The presence of deep conductive region (<75 ohm m) at a depths ~15 km and ~35 km indicates the heat source of geothermal system developed around Kizildere area.

It is interesting that deep conductive zones are situated on the eastern part of B. Menderes Graben where it intersects with Çürüksu and Gediz Grabens.

REFERENCES

Enel, Aquater and Geotermica Italiana, 1988. "Optimization and Development of teh Kızılıdere geothermal Field", Appendix 5 Integrative Prospectings Magnetotelluric Report, Pisa Italy.

Berdicehevsky, M.N., Dimitriev, V.I., and Pozdnjakova, E.E., 1998. "On two-dimensional interpretation of magnetotelluric soundings". *Geophys. J. Int.*, 133, 585-606.

Dominco, E. and Samilgil, E., 1970. "Geochmistry of the Kizildere Geothermal Field, in the Framework of the Sarayköy-Denizli Geothermal Area", UN symposium on Development and Utilization of Geothermal Resources, Vol. 2, Part 1, Pisa.

Harinarayana, T., Azeez, K.K.A., Naganjaneyulu, K., Manoj, C., Veeraswamy, K., Murthy, D.N., and Rao, S.P.E., 2004. "Magnetotelluric studies in Puga valley geothermal field, NW Himalaya, Jammu and Kashmir, India", *Journal of Volcanology and Geothermal Research*, 138, 405-424.

Ilkisik, O.M., 1995. "Regional heat flow in western Anatolia using silica temperature estimates from thermal springs". Tectonophysics 244, 175-184.

Mackie, R., Rieven, S., and Rodi, W., 1997. "Users Manual and Software Documentation for Two-Dimensional Inversion of Magnetotelluric Data", GSY-USA Inc., California, 14 Pages.

MTA, 1964, "Geological map of Turkey, scale1:1000000 Denizli sheet". Institute of Mineral Research and Exploration, Ankara.

Lugão, P.P., LaTerra, E.F., Kriegshäuser, B., and Fontes, S.L., 2002. "Magnetotelluric Studies of the Caldas Novas geothermal reservoir, Brazil", *Journal of Applied Geophysics*, 49, 33-46.

Rodi, W. and Mackie, L.R., 2001. "Nonlinear conjugate gradients algorithm for 2-D magnetotelluric inversion", *Geophysics*, 66, 174-187.

Wannamaker, P.E., Booker, J.R., Filloux, J.H., Jones, A.G., Jiracek, G.R., Chave, A.D., Tarits, P.,

Waff, H.S., Egbert, G.D., Young, C.T., Stodt, J.A., Martinez, M., Law, L.K., Yukutake, T., Segawa, J.S., White, A., and Green, A.W., 1989. "Magnetotelluric observations across the Juan de Fuca subduction system in the EMSLAB project", *J. Geophys. Res*., 94, 14111-14125.